J. Phycol. **46,** 456–465 (2010)

DOI: 10.1111/j.1529-8817.2010.00821.x

CELL-WALL POLYMER MAPPING IN THE COENOCYTIC MACROALGA *CODIUM VERMILARA* (BRYOPSIDALES, CHLOROPHYTA)[1]

Paula V. Fernández, Marina Ciancia[2]

Cátedra de Química Orgánica, Departamento de Biología Aplicada y Alimentos (CIHIDECAR-CONICET), Facultad de Agronomía, Universidad de Buenos Aires, Av. San Martín 4453, C1417DSE Buenos Aires, Argentina

Alicia B. Miravalles

Departamento de Biología, Bioquímica y Farmacia, Universidad Nacional del Sur, 8000 Bahía Blanca, Argentina

and José Manuel Estevez[2,3]

Departamento de Fisiología, Biología Molecular y Celular (IFIByNE-CONICET), Facultad de Ciencias Exactas y Naturales, Universidad de Buenos Aires, Ciudad Universitaria – Pabellón 2, 1428 Buenos Aires, Argentina

Cell walls in the coenocytic green seaweed *Codium vermilara* (Olivi) Chiaje (Bryopsidales, Chlorophyta) are composed of ~32% (w/w) β-(1 → 4)-D-mannans, ~12% sulfated polysaccharides (SPs), and small amounts of hydroxyproline-rich glycoprotein-like (HRGP-L) compounds of the arabinogalactan proteins (AGPs) and arabinosides (extensins). Similar quantities of mannans and SPs were reported previously in the related seaweed *C. fragile* (Suringar) Hariot. Overall, both seaweed cell walls comprise ~40%–44% of their dry weights. Within the SP group, a variety of polysaccharide structures from pyruvylated arabinogalactan sulfate and pyruvylated galactan sulfate to pyranosic arabinan sulfate are present in *Codium* cell walls. In this paper, the in situ distribution of the main cell-wall polymers in the green seaweed *C. vermilara* was studied, comparing their arrangements with those observed in cell walls from *C. fragile*. The utricle cell wall in *C. vermilara* showed by TEM a sandwich structure of two fibrillar-like layers of similar width delimiting a middle amorphous-like zone. By immuno- and chemical imaging, the in situ distribution of β-(1 → 4)-D-mannans and HRGP-like epitopes was shown to consist of two distinct cell-wall layers, whereas SPs are distributed in the middle area of the wall. The overall cell-wall polymer arrangement of the SPs, HRGP-like epitopes, and mannans in the utricles of *C. vermilara* is different from the ubiquitous green algae *C. fragile*, in spite of both being phylogenetically very close. In addition, a preliminary cell-wall model of the utricle moiety is proposed for both seaweeds, *C. fragile* and *C. vermilara*.

Key index words: **carbohydrate immunolabeling; cell-wall arrangement; chemical imaging; *Codium vermilara*; coenocytic green seaweed; hydroxyproline-rich glycoprotein-like; SR–FTIR microspectroscopy; sulfated polysaccharides; β-(1 → 4)-D-mannans**

Abbreviations: **AGPs, arabinogalactan proteins; HRGP-L, hydroxyproline-rich glycoprotein-like; IDA, immuno dot-blot assay; LSCM, laser scanning confocal microscopy; SP, sulfated polysaccharide; SR–FTIR, synchrotron radiation–Fourier transform infrared; TB*O*, toluidine blue *ortho*chromatic; TFA, trifluoroacetic acid**

Most siphonous green seaweeds, such as *Codium*, *Bryopsis*, and so forth, are macroalgae belonging to the order Bryopsidales (Chlorophyta). The seaweeds in the Bryopsidales group are also called ''giant single cell'' algae because the habit comprises continuous siphons, which lack cross cell walls, and septa are formed only at the time of differentiation of reproductive structures. These taxa constitute a vital component of coral reefs throughout the world and have successfully maintained their ecological niches and persisted for >150 million years (Hay 1997). The genus *Codium* is very diverse, comprising ~156 taxonomically accepted species (Guiry and Guiry 2009) with a variety of morphologies that span the temperate and tropical zones of the globe (Verbruggen et al. 2007). Four species of *Codium* grow in the Argentine littoral: *Codium fragile* subsp. *novae-zelandiae*, *C. vermilara*, *C. decorticatum*, and *C. subantarcticum* (Boraso de Zaixso 2004).

Cell walls in all macroalgae and especially in the coenocytic seaweeds are the first means of defense against variety of factors, such as wave action, water currents, pressure changes, osmotic changes, epiphytic load, herbivore attack, and invasion by

[1]Received 16 April 2009. Accepted 18 November 2009.
[2]Research Member of the National Research Council of Argentina (CONICET).
[3]Author for correspondence: e-mail jestevez@fbmc.fcen.uba.ar.

pathogens (Ram and Babbar 2002). *Codium* has developed completely different cell walls when compared with all cellulose-rich walls present in land plants and in other green algae (Bilan et al. 2007, Ciancia et al. 2007, Farias et al. 2008, Popper 2008, Estevez et al. 2009). It was shown previously that *C. fragile* and *C. vermilara* from Argentinian coasts biosynthesize major amounts of β-(1 → 4)-D-mannans and intermediate percentages of SPs (Ciancia et al. 2007, Estevez et al. 2009). SP in both seaweeds comprises several diverse polysaccharide structures: (1) pyruvylated arabinogalactan sulfates, containing sulfated groups at C-2 and/or C-4 of the 3-linked β-L-Ara*p* units and at C-4 and/or C-6 of the 3-linked β-D-Gal*p* residues (in addition, high levels of ketals of pyruvic acid were found mainly linked to C-3 and C-4 of some terminal β-D-Gal*p* units forming a five-membered ring); (2) pyruvylated galactan sulfates composed of 3-linked β-D-Gal*p* residues with sulfated groups on C-4 or substituted at C-4 and C-6 and 4,6-pyruvylated; and (3) pyranosic arabinan sulfates with 3-linked β-L-Ara*p* 2,4-disulfate units and 3-linked β-L-Ara*p* 4-sulfate residues. The ratio between these structures is variable according to the species (Bilan et al. 2007, Ciancia et al. 2007, Farias et al. 2008, Estevez et al. 2009). In addition, small amounts of HRGP-L epitopes were shown in *C. fragile* cell walls (Estevez et al. 2009). Recently, it was shown that *C. isthmocladum* and *C. yezoense* biosynthesize pyruvylated galactan sulfates with similar structural features (Bilan et al. 2007, Farias et al. 2008).

The spatial arrangement of the cell-wall polymers in green algae remains mostly uncharacterized, with the exception of simple models, such as those of volvocacean and desmid algae, and also the more complex walls of the green seaweed *Ulva* (Domozych and Domozych 1993, Bobin-Dubigeon et al. 1997, Ender et al. 2002, Hallmann 2006, Domozych et al. 2009). Taking advantage of the existing detailed knowledge on the chemistry of cell-wall polymers present in *Codium* in recent years (Bilan et al. 2007, Ciancia et al. 2007, Farias et al. 2008, Estevez et al. 2009), the in situ distribution of β-(1 → 4)-D-mannans and SPs together with HRGP-L epitopes in *C. vermilara* was further characterized and compared with their arrangements in the walls from *C. fragile*. In addition, a preliminary model of the utricle cell wall is proposed for both *C. vermilara* and *C. fragile*.

MATERIALS AND METHODS

All chemicals were purchased from Sigma Inc. (St. Louis, MO, USA), unless otherwise stated. JIM11, JIM16, JIM20, LM1, and MAC206 antibodies were purchased from PlantProbes (Leeds, UK), and a monoclonal antibody against β-(1 → 4)-D-mannan was purchased from Biosupplies (Parkville, Australia). Chemical synthesis of β-GlcYR and α-ManYR was carried out as described in Yariv et al. (1962) and tested against gum arabic in a dot-blot assay.

Algal sample. Thalli of *C. vermilara* were collected in Puerto Madryn, Province of Chubut (42°46′ S, 65°03′ W). A voucher material was deposited in the herbarium of the Museo Bernardino Rivadavia (B.A.), Buenos Aires, Argentina (collection number 40466).

In situ immunolocalization. The algal material was fixed in 4% formaldehyde, dehydrated in EtOH series, and embedded in paraplast (Fisher, Pittsburgh, PA, USA). Cross-sections of 10 μm were collected on ProbeOn microscope slides (Fisher), and after removal of the resin with histoclear, they were blocked in PBS containing 5% (w/v) fat-free milk powder (5% modified phosphate-buffered saline, MPBS) for 30 min. Rat monoclonal antibodies specific for carbohydrate epitopes were used: arabinosides of the extensin-like type (JIM11 and JIM20, Smallwood et al. 1994) and AGP-like glycans (JIM16, Knox et al. 1991; MAC207, Yates et al. 1996). The primary antibody (dilution 1:50–1:500) was incubated 1 h at room temperature and washed with PBS (2X). For visualizing the antibody binding, a secondary antibody antirat-IgG coupled with Alexa Fluor 488 (Molecular Probes, Carlsbad, CA, USA) (1:1,000) in 5% MPBS was added for 1 h at room temperature. After washing with PBS for 5 min (2X), the samples were observed in a laser scanning confocal microscope (LSCM, see below). To localize the β-(1 → 4)-D-Man*p* units, a specific antimannan polyclonal antibody (Mab) developed by Handford et al. (2003) was used (dilution 1:100). As a secondary antibody, an antirabbit-IgG coupled with Alexa Fluor 565 (Molecular Probes) (dilution 1:250) was used. Primary antibodies, which were omitted for labeling procedure, acted as first control for all the immunolocation probes. Additionally, preextracted sections, where soluble AGPs and extensins were removed, were visualized as before. As an additional negative control, nonextracted and nonlabeled sections were visualized in the same conditions as before to check the presence of intrinsic autofluorescence coming from the algal material.

LM and histochemistry. For LM, sections (~10 μm) were mounted on glass slides and then observed with a Carl Zeiss Axiolab microscope (Carl Zeiss, Jena, Germany). The staining procedures used in LM histochemical characterization, based on Krishnamurthy (1999), were carried out on fixed tissues described before and included: (1) toluidine blue *O* (TB*O*) (0.05% w/v) in 0.1 M HCl at pH 1.0 that stains SPs (red-purple, γ metachromasia). As a negative control, the labeling with TB*O* on preextracted sections was performed to remove the SPs using the same conditions as before. (2) Calcofluor white (CW) (0.1% w/v) in aqueous solution for detection of β-(1 → 3)- and β-(1 → 4)- polysaccharides. In addition, β-Glc Yariv phenylglycoside reagent (β-GlcYR) was used for localized AGPs due to its specificity, and α-Man Yariv phenylglycoside reagent (α-ManYR) was used as a negative control. Sections of the thallus were incubated overnight with 1% Yariv derivatives (w/v) at 4°C in 1% in NaCl (w/v) solutions and then washed three times in 1% in NaCl (w/v). Preextracted sections were incubated with water at 90°C for 2 h to remove mostly water-soluble SPs and water-soluble HRGPs.

TEM. Utricles were fixed in 2% glutaraldehyde in 0.1 M cacodylate buffer, postfixed in 1% OsO_4, dehydrated in an acetone series, and embedded in Spurr's low viscosity resin (Spurr 1969). Sections were cut using a diamond knife (Diatome Ltd., Bienne, Switzerland) and stained with uranyl acetate and lead citrate. Sections were observed using a JEOL 100 CX-II electron microscope (JEOL, Akishima, Tokyo, Japan).

Carbohydrate immunodot-blot assays (IDAs). Two microliters of the water-diluted cell-wall extracts and residues at different concentrations from 1 to 4 $\mu g \cdot \mu L^{-1}$ was applied into nitrocellulose membranes. After drying the membrane for 30 min, blots were blocked with 5% MPBS for 1–2 h. The primary antibody was used in variable concentration (1:50 to 1:1,000) in

5% MPBS during 3 h. After washing with TTBS (tween 0.05% [v/v] in 1X PBS) twice and once with 1X PBS, blots were incubated under the secondary antibody antirat IgG coupled to AP (alkaline phosphatase) for 1 h. After washing as described before, the blots were developed in 5-bromo-4-chloro-3-indolyl phosphate (BCIP) and nitroblue tetrazolium (NBT) for <10 min at room temperature until color reaction was observed. The experiment was repeated twice. See Estevez et al. (2009) for specificity of antibodies. Gum arabic was used as a positive control for the anti-HRGP antibodies used in this study.

Electrophoresis and Western blot analysis. Agarose gel electrophoresis was performed in a 1% (w/v) gel poured in 1X TBE buffer (0.045 M Tris-borate, 0.001 M EDTA). Eighty micrograms of each sample was loaded in the gel, and constant current (40 mV) was applied for 60 min. For Western blot analysis, 200–300 μg of sample was solubilized in 50 μL of 2X Laemmli buffer (125 mM Tris-Cl, pH. 6.8, 4% [w/v] SDS, 20% [v/v] glycerol, 2% [v/v] β-mercaptoethanol, 0.001% [w/v] bromophenol blue) containing 10 μL protease inhibitor cocktail (Sigma) and immediately transferred to ice. The samples were boiled for 5 min, and 15–20 μL was loaded on 4%–20% SDS-PAGE. In all the cases, the HRGP-L epitopes were separated by electrophoresis and transferred to nitrocellulose membranes. Rat IgG antibodies for AGPs (JIM16) and extensins (JIM20) recognition were used at dilutions of 1:500 and visualized by incubation with antirat IgG secondary antibodies conjugated to horseradish peroxidase (1:1,000) followed by a chemiluminescence reaction (Super-Signal; Pierce Chemical, Rockford, IL, USA). See Estevez et al. (2009) for specificity of antibodies. The same samples were loaded into 4%–20% SDS-PAGE and run using the same conditions described before. SPs were visualized with 1% (w/v) TB*O* (pH = 1.0). Migration patterns of SPs and AGP glycans in the SDS-PAGE and nitrocellulose membranes, respectively, were analyzed using Image J 1.34 software (http://rsb.info.nih.gov/ij/), and the images were processed with Adobe Photoshop 7.0 (Adobe Systems, Mountain View, CA, USA).

Enzymatic treatments. In situ β-mannanase treatments were performed over semithin sections obtained from *C. vermilara* after removal of paraplast resin. Sections were incubated with an endo-β-(1 → 4)-D-mannanase (AN3358.2; Bauer et al. 2006) in 50 mM acetate buffer pH 5.5 at 37°C overnight. The buffer without the enzyme was used as a control. The solution was carefully recovered from 40 sections, and the content in mannose units released after the treatment was determined as alditol acetates and was expressed per cross-section area. Cross-section area was measured using Image J 1.36b software. Analysis of residue obtained after hot-water extractions (RW2) by carbohydrate gel electrophoresis was performed as described in Estevez et al. (2009).

Chemical analysis. Chemical analyses were performed as described in Ciancia et al. (2007) and Estevez et al. (2009). In addition, the total carbohydrate content of RW2 was analyzed by a phenol–sulfuric acid method adapted for insoluble material (Ahmed and Labavitch 1977). To determine the monosaccharide composition of the RW2 fraction, the sample (3 mg) was dissolved in 100% trifluoroacetic acid (TFA: 37°C, 1 h), followed by dilution of the acid to 80%, heating at 100°C for 1 h, and further dilution to 2 M to achieve the regular hydrolysis conditions, reduction with $NaBH_4$, and acetylation (Morrison 1988). Sulfate was determined, after hydrolysis of the sample, by ionic isocratic chromatography on a Dionex DX-100 apparatus equipped with a Dionex AS4A column (Dionex Corporation, Sunnyvale, CA, USA) and using a Na_2CO_3 1.8 mM, $NaHCO_3$ 1.7 mM solution as eluant. The pyruvic acid content was estimated by the method of Koepsell and Sharpe (1952). To quantify the mannan content present in cell wall, the total carbohydrate content (TC), measured in the cell-wall extracts V1-V2 and W1-W2, and in residue RW2, was corrected by the amount of mannose determined as alditol acetate. This estimate was used to quantify the total yield of mannan. In the same way, the amount of sulfated polymers was estimated by the sum of TC (including only arabinose and galactose sugars) plus sulfate and pyruvic acid contents. The value obtained was used to correct the yield of SP.

Fourier transform infrared (FTIR) and synchotron radiation–Fourier transform infrared (SR–FTIR) microspectroscopy. Fourier transform infrared spectra were recorded from 4,000 to 250 cm^{-1} with a 510P Nicolet FTIR spectrophotometer (Madison, WI, USA), using dry samples in KBr. Sixty-four scans were taken with a resolution of 2 cm^{-1}. For SR–FTIR microspectroscopy, *Codium* samples already embedded in paraplast were cut into thin sections (~10 μm) with a microtome (C. Reichert Optische Werke, Wien, Austria), and then paraplast resin was removed with histoclear. Cross-sections were transferred to low e-microscope slides (MirrIR, Kevley Tech, Chesterland, OH, USA) and FTIR reflection spectra (also called as ''double absorption'' mode) were acquired at the infrared spectromicroscopy beamline 1.4.3 at the Advance Light Source (ALS, Berkeley, CA, USA). The synchrotron light was used as an external source for a Nicolet 760 FTIR bench and Nic-PlanTM microscope to perform reflection microscopy with a computer-controlled *x-y-z* sample stage. The beamline only allows light between 400 and 10,000 cm^{-1} to continue on to the sample with diffraction-limited spot (3–10 μm diameter) with high brightness (1.3×10^{-2} mW · μm^{-2}). Brightness refers to photon flux (unit area)$^{-1}$ · (unit bandwidth)$^{-1}$ · (solid angle)$^{-1}$. For cell-wall mapping, 96 spectra were recorded over the region from 650 to 4,000 cm^{-1} with a spectral resolution of 4 cm^{-1}, Happ-Genzel apodization, and 64 scans co-added for Fourier transform processing to produce one spectrum. A background spectroscopic image file was collected from an area free of sample. Stage control, data collection, and processing were performed on the OMNIC 7.2 (Thermo-Nicolet, Madison, WI, USA) together with Win-Das software (Wiley, New York, NY, USA). Spectra were first baseline corrected and area normalized to compensate for any change in thickness across the section.

RESULTS AND DISCUSSION

C. vermilara is characterized by the complex interwoven multiaxial siphon pattern with a solid and cylindrical frond, which has a central colorless medulla with coenocytic filaments and an external palisade cortex composed of enlarged utricles with rounded apical endings (Fig. 1, a and b). The utricle cell wall shows an external cuticle and two fibrillar-like layers (fl) delimiting a middle amorphous layer (al) (Fig. 1c). A similar utricle cell-wall structure was confirmed by TEM, with an external cuticle, two electrodense fibrillar-like layers, and a central amorphous layer (al) (Fig. 1, d and e). To reveal the in situ localization of the main polymers in *C. vermilara* cell walls (β-mannans, SPs, and HRGP-like epitopes), both immunolabeling and chemical imaging approaches were used.

β-(1 → 4)-D-mannans. The presence of mannans with β-(1 → 4)-linkages was previously confirmed by linkage and NMR analysis made on isolated cell-wall polymers (Ciancia et al. 2007). Here, we used calcofluor white (CW) staining (Krishnamurthy 1999), birefringence detected by phase contrast, and

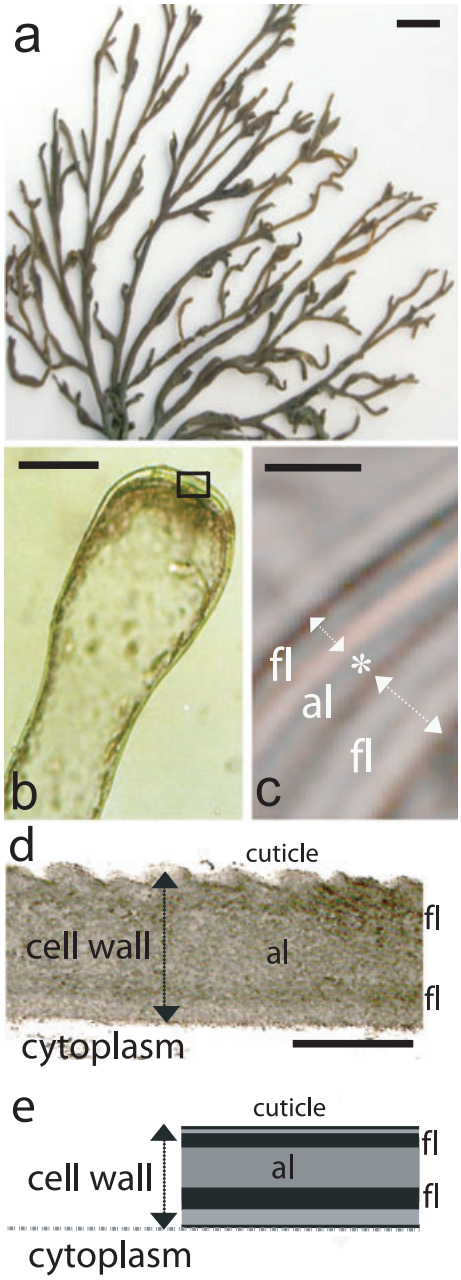

FIG. 1. General aspect of the thallus of *Codium vermilara* (a) Scale bar = 1cm. (b) Coenocytic structure of a single utricle cell. Scale bar = 150 µm. (c) Utricle cell wall by LM. Scale bar = 10 µm. (d) Utricle cell-wall structure is visualized in detail by TEM. An external cuticle, two electrodense fibrillar-like layers (fl), and a central amorphous layer (al) are clearly distinguished. Scale bar = 20 um. (e) Scheme of the utricle cell-wall structure in *C. vermilara*.

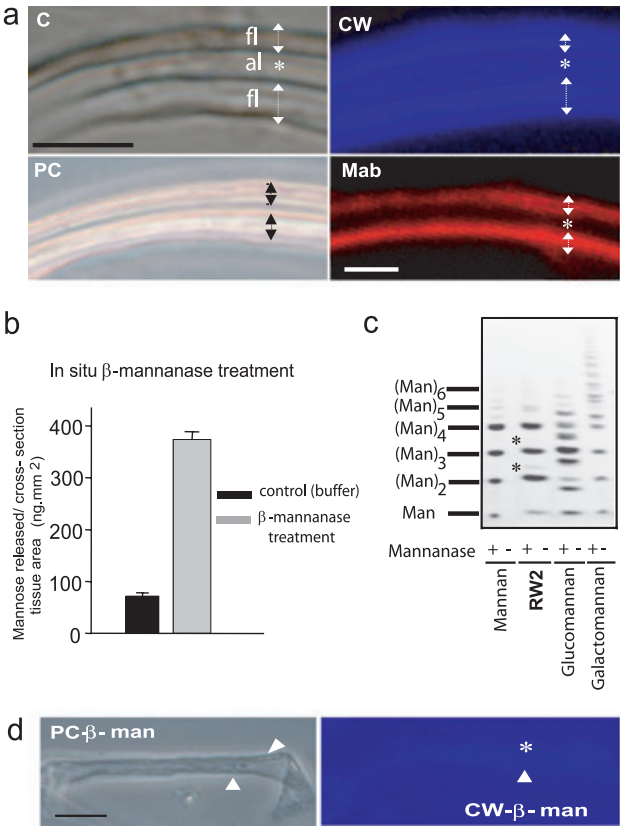

FIG. 2. In situ distribution of β-(1 → 4)-D-mannans in *Codium vermilara* cell walls. (a) Double two fibrillar (arrows) and amorphous (*) cell-wall strata of the utricle from *C. vermilara* in longitudinal section observed with light-directed (C) and phase contrast (PC) microscopy. In addition, calcofluor white staining (CW) and labeling of β-(1 → 4)-D-mannosyl units with an antimannan antibody (Mab) were used to localize the β-(1 → 4)-D-mannans in the cell wall (bottom). Outer and inner cell-wall limits are indicated with arrowheads. Scale bar = 20 µm. (b) In situ mannanase treatment of the cell walls. Sugars released per cross-section area of the whole thalli after in situ β-mannanase treatment (ng mannose · mm^{-2}) compared with buffer incubation used as a control (left). Forty cross-sections were used for each treatment. (c) Algal cell-wall mannan derived from RW2 (~87 mol% mannose) was analyzed by carbohydrate gel electrophoresis, using the endomannanase Man5A. The main products of the digestion were mannose, mannobiose, mannotriose, and mannotetraose. Two minor bands (*) were also detected suggesting some small degree of substitution on the mannan backbone. Oligosaccharides released from 1.25 µg of digested cell walls or 0.5 µg standard digested polysaccharides are shown. (d) Phase contrast microscopy and CW staining after in situ β-mannanase treatment (PC- and CW-β-man, respectively). Scale bar = 40 µm. The presence (arrowhead) and absence (*) of β-(1 → 4)-D-mannans before and after mannanase treatment is indicated. al, amorphous layer; fl, fibrillar layer; RW2, residue obtained after hot-water extractions.

antibody labeling for β-(1 → 4)-D-mannosyl units to show the in situ localization of β-(1 → 4)-D-mannans in the cell walls of *C. vermilara* (Fig. 2a). This polymer is localized into two well-defined cell-wall layers with similar development and separated by one nonreactive major zone (Fig. 2a).

An in situ enzymatic treatment using a specific mannanase, which hydrolyzes only β-(1 → 4)-D-mannosyl units, was performed on cross-sections and also on the residue obtained after exhaustive water extraction of the seaweed cell walls with RW2 (Figs. 2, b–d) to confirm the labeling results. The quantity of mannose units released after enzymatic

degradation (Fig. 2b) was significantly higher in the mannanase-treated sections (480 ± 10 ng mannose · mm^{-2}) than in the control (80 ± 5 ng mannose · mm^{-2}). After enzymatic treatment on the cross-sections, CW staining (CW β-ManT, Fig. 2d) was very low on the cell walls. Furthermore, not only the ordered fibrillar arrangement was lost (with negative or weak birefringence), but also some cell-wall areas were severely damaged, suggesting a possible putative major structural role for the β-(1 → 4)-D-mannans as scaffold in these cell walls as it was shown previously for *C. fragile* (Estevez et al. 2009).

In addition, an oligosaccharide analysis by carbohydrate gel electrophoresis was carried out on the product obtained by enzymatic degradation from RW2 (Fig. 2c). RW2 is composed of 69% carbohydrates, from which 87 mol% is mannose and comprises 50% (w/w) dry seaweed weight (Table S1 in the supplementary material). These cell-wall-derived oligosaccharides were compared to oligosaccharides obtained from commercial mannans, glucomannans, and galactomannans that had been hydrolyzed by the same enzyme, used as standards. The main products from RW2 digestions were mannose, mannobiose, mannotriose, and mannotetraose that migrated exactly as those derived from the commercial β-(1 → 4)-D-mannan (Fig. 2c). This finding indicates that mannans are mostly composed of a repetitive [→ 4)-β-D-mannosyl-(1 →] structure, although some small degree of substitution was suggested by two minor bands in the carbohydrate gel electrophoresis analysis (Fig. 2c) as it was previously indicated by chemical methods (Ciancia et al. 2007).

Mannan polysaccharides are widespread among land plants, where they serve as structural elements in cell walls and as carbohydrate reserves and potentially perform other important functions (Liepman et al. 2007). The presence of β-(1 → 4)-D-mannans as the major structural cell-wall polysaccharide in *Codium* and β-(1 → 3)-D-xylans in other close coenocytic green seaweeds (i.e., *Bryopsis* and *Caulerpa*) (Chanzy et al. 1984, Fukushi et al. 1988) instead of cellulose, shows that this unique group of organisms has more than one way to develop distinct cell walls within coenocytic thalli. Likewise, in *Bryopsis,* where gametophytic cells have been reported to produce only fibrillar β-(1 → 3)-D-xylans and the sporophytic ones biosynthesize β-(1 → 4)-D-mannans (Huizing et al. 1979), a hybrid protoplast with both gametophytic and sporophytic nucleus synthesizes only β-(1 → 4)-D-mannans. The gametophytic nucleus seems to repress the genes coded in the coexisting sporophytic one that are involved in xylan synthesis (Yamagishi et al. 2004). Recently, several mannan synthases were identified as cellulose-synthase-like A (Csl*A*) gene family of glycosyltransferases that make β-(1 → 4)-D-mannans in many land plant groups ranging from mosses to angiosperms (Dhugga et al. 2004, Liepman et al. 2005, 2007). Identification and expression analysis of Csl*A*- and others Csl-gene families in seaweeds from the Bryopsidales group may also provide insights into the evolutionary origins of these complex and unique cell walls.

SPs. Using synchrotron radiation-based midinfrared (SR-IR) spectroscopy coupled to a microscope (SR–FTIR microspectroscopy), it was possible to map the SPs present on the cell wall of the utricle tip (Fig. 3a). Absorbance bands at 1,380 cm^{-1}, common for all sulfate esters, at 1,230–50 cm^{-1} that correspond to the asymmetric stretching of the O=S=O, together with absorbance at 850 cm^{-1} for $C–O–SO_3^-$ as secondary axial sulfate and 820–30 cm^{-1} for $C–O–SO_3^-$ as primary sulfate were identified (Prado Fernandez et al. 2003) using as a reference the FTIR spectrum of V1, the room-temperature water extract obtained from this seaweed (Fig. S1 in the supplementary material). V1 shows a high level of sulfate groups (30% w/w of

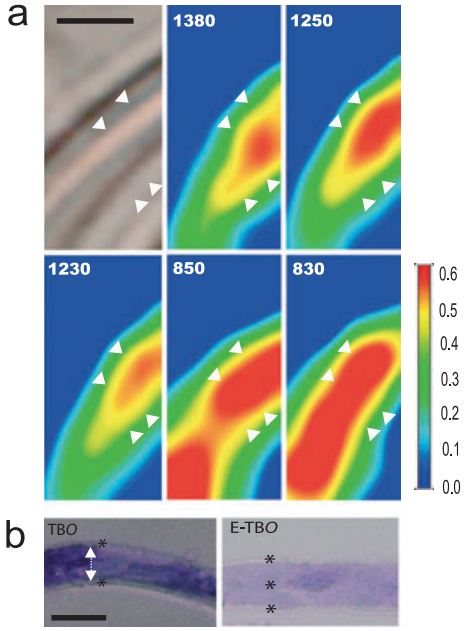

FIG. 3. Localization of sulfated polysaccharides (SPs) in the cell wall from *Codium vermilara* assessed by synchrotron radiation–Fourier transform infrared microscopy (SR–FTIR microspectroscopy) (a) and by histochemistry with toluidine blue *O* (TB*O*) (b). (a) Chemical images using SR–FTIR microspectroscopy of a longitudinal section of the cell-wall area from the utricle tip. Specific absorption band intensity map corresponding to ester sulfate bands (1,380, 1,250, and 1,230 cm^{-1}) and at 850 cm^{-1} associated to axial $C–O–SO_3^-$ (secondary axial sulfate) and at 820–30 cm^{-1} ($C–O–SO_3^-$, primary sulfate) are shown. All of them showed a similar pattern with maximum absorbance in the amorphous central zone. Arrowheads were included to show the limit of the middle amorphous cell-wall area. Scale bar = 20 μm. (b) Negative-charged sulfate groups present in the SPs were labeled with TB*O* at pH = 1. Preextracted sections, where SPs were mostly removed, showed much lower labeling with TB*O* at the same condition used before (E-TB*O*). Most reactive cell-wall areas are indicated with arrowheads. On the other hand, absence of labeling is shown with asterisks. Scale bar = 30 μm.

sulfate) and only 2% of mannose (Table S1). Sulfate groups on the SPs were present in V1 mainly linked to C-2 and C-4 of the 3-linked Ara*p* units and on C-4 of the 3,6-linked Gal*p* residues (Ciancia et al. 2007). These absorbance bands were used to map the in situ distribution of sulfate groups present in SPs on the utricle cell wall (Fig. 3a). The pattern of distribution for most of the sulfate-associated bands on the SR–FTIR microspectroscopy scanning map showed a location of SPs on the middle amorphous-like layer (Fig. 3a). In addition, negatively charged sulfate groups were labeled with TB*O* at pH = 1 (Krishnamurthy 1999) showing a similar staining pattern (Fig. 3b). Preextracted sections, where SPs were mostly removed, showed very low labeling with TB*O* on the amorphous-like layer (E-TB*O*; Fig. 3b).

SPs are widespread in the cell walls from several marine organisms, including all groups of seaweeds, marine angiosperms (Les et al. 1997, Stortz and Cerezo 2000, Ponce et al. 2003, Estevez et al. 2004, Aquino and Landeira-Fernandez 2005), and also in extracellular matrices of invertebrate ascidians and echinoderms (Santos et al. 1992, Vilela-Silva et al. 2002). In all these organisms, the SPs that are strongly charged in seawater media would act as ionic and osmotic regulators, providing hydration by gel formation and mechanical stress resistance in wave-swept intertidal habitats (Kloareg and Quatrano 1988). Convergent evolution was suggested as a putative, and the most probable, mechanism to explain the fact that all these phylogenetically distant organisms possess structurally related SPs in their cell-wall intercellular matrices (Aquino and Landeira-Fernandez 2005).

HRGP-L polymers. Previously, HRGP-L epitopes were detected in the cell wall of *C. fragile* (Estevez et al. 2009). To determine if HRGP-L epitopes are also present in *C. vermilara*, most of the available antibodies against plant HRGP were tested by immunodot-blot assay (IDA) on isolated cell-wall fractions (Fig. S2 in the supplementary material). Strong reaction was detected in most of these cell-wall fractions using anti-AGPs (JIM16 and MAC207) and antiextensin probes (JIM11, JIM20, and LM1) (Fig. S2). In addition, the amino acid analysis showed that 30–40 mol% of the proline units were hydroxylated at C-4, giving Hyp in the room-water extracts V1-V2 (not shown). These results confirm the presence of HRGP-L in the cell walls of *C. vermilara*. Since proteoglycans detected in *Codium* react with several monoclonal antibodies generated against AGPs and extensins from cell walls of higher plants, we refer to them as ''HRGP-like.'' The purification and characterization of *O*-glycan structures and protein backbones present on the HRGP-L of *C. vermilara* walls are currently under investigation.

To address if the sulfate groups are present only in SP or also in the AGP and/or extensin epitopes, the main water-soluble cell-wall extracts (V1-V2, Table S1) were analyzed by SDS-PAGE

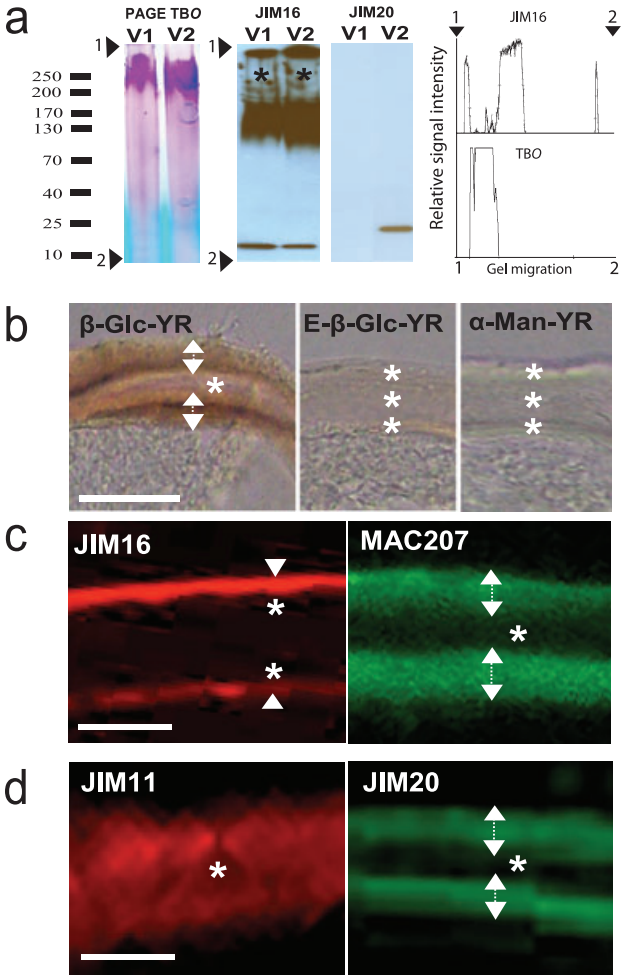

FIG. 4. SDS-PAGE and immunolocalization of HRGP-L epitopes in the cell walls of *Codium vermilara*. (a) SDS-PAGE analysis of the sulfated polysaccharides (SPs) with toluidine blue *O* (TB*O*) staining (left), whereas AGP glycans are visualized by JIM16 labeling and extensin epitopes by JIM20 by Western blot on a nitrocellulose membrane (center). Only water-soluble cell-wall components (extracts V1-V2) are shown. In addition, PAGE and Western blot profiles of the SP and HRGP-L epitopes from V1, respectively, were analyzed with Image J (right). Loading sites of these samples are shown by an arrowhead (see Materials and Methods). No detectable overlapping was found between sulfated groups and HRGP-L epitopes. (b) In situ AGP labeling. Positive β-glucosyl Yariv-staining (β-Glc-YR) indicates the presence of AGP epitopes in the cell walls. Preextracted sections were labeled, and most of the signal was lost (E-β-Glc-YR). In addition, negative α-mannosyl Yariv-staining (α-Man-YR) was observed in the preextracted sections. Scale bar = 30 μm. (c) In situ immunolocalization by laser scanning confocal microscopy (LSCM) of AGP-like epitopes with JIM16 and MAC206 antibodies (Knox et al. 1991 and Yates et al. 1996, respectively) in the cell wall of *C. vermilara*. Utricles in longitudinal-section view (middle panels). Scale bar = 20 μm. (d) Extensin-like epitope labeling with JIM11 and JIM20 antibodies (Smallwood et al. 1994). Scale bar = 20 μm. In all cases, the most reactive cell-wall areas are indicated with arrowheads. On the other hand, absence of labeling is shown with asterisks. HRGP-L, hydroxyproline-rich glycoprotein-like.

(Fig. 4a). Strong TB*O*-labeling bands were detected (Fig. 4a) in agreement with the high sulfate content (Ciancia et al. 2007 and Table S1). Based on the

immunoassays, bands corresponding to AGPs are also present in most of the cell-wall fractions, but their SDS-PAGE migration profiles do not overlap with TBO-staining patterns of the SPs (Fig. 4a). These results indicate that HRGP-L epitopes and SPs in V1-V2 are mostly different cell-wall components. At least three groups of AGP epitopes were identified with JIM16 based on the migration on PAGE gels (Fig. 4a), two of high molecular mass (>250 and ~110–180 kDa) and another of ~12 kDa. In addition, an extensin epitope was also detected (~20 kDa) only in the V2 fraction. An overestimation of molecular mass on Western blots for AGP epitopes is expected due to the poor mobility of the highly *O*-glycosylated proteins in SDS gels due to the steric hindrance of SDS binding to the polypeptide backbone (Hames and Rickwood 1990, Estevez et al. 2006).

β-Glucosyl Yariv phenylglycoside reagent (β-GlcYR), known to specifically bind AGPs in a noncovalent manner (Yariv et al. 1962), was used to localize the entire population of AGPs in the cell walls of *C. vermilara* (Fig. 4b). β-GlcYR labeling was detected in two marginal cell-wall layers, whereas sections incubated with α-mannosyl Yariv phenylglycoside (α-ManYR), which were used as negative control, remained unreactive (Fig. 4b). In addition, AGP epitopes were detected with JIM16 and MAC207 antibodies showing a similar two-layered wall distribution with broader labeling in the fibrillar-like zones for MAC207 (Fig. 4b) as it was shown with β-GlcYR (Fig. 4b). Preextracted sections, where most of the soluble HRGP-L epitopes were removed, showed a much lower signal or no signal when incubated with β-GlcYR (Fig. 4b) or with all the antibodies against HRGP-L epitopes (not shown). JIM16 and MAC207 antibodies recognize the carbohydrate moiety of AGP epitopes on molecules that are largely uncharacterized (Knox et al. 1991, Yates et al. 1996). It is likely that either similar AGP epitopes are present on many AGPs with different protein backbones, or only a few epitopes restricted to specific AGPs were recognized with these two antibodies. Arabinoside epitope (extensins) localization, shown by JIM11 and JIM20 labeling (Fig. 4c), followed a pattern similar to that observed for the AGP molecules. Results obtained using these antibodies (Smallwood et al. 1994) indicate that both *C. vermilara* and *C. fragile* (Estevez et al. 2009) contain extensin-like epitopes as do higher plants (Knox et al. 1991) and the green alga *Chlamydomonas* (Hicks et al. 2001), whereas these same epitopes were absent in the cell walls of *Micrasterias* (Eder et al. 2008).

Immunocytochemical and chemical evidence suggests that the cell-wall AGPs occur not only in most land plants but are also widespread among diverse groups of green algae, including phylogenetically distant marine seaweeds (*Codium*) and freshwater micro- and macroalgae groups (*Chara*, *Chlamydomonas*, *Micrasterias*, *Oedogonium*, *Pleurotaenium* Nägeli) (Lutz-Meindl and Brosch-Salomon 2000, Ender et al. 2002, Popper and Fry 2003, Hallmann 2006, Domozych 2007, Ender et al. 2008, Estevez et al. 2008, 2009). The presence of AGPs in green algae and land plants suggests at least some putative essential biological roles possibly associated with a well-conserved carbohydrate domain present on these *O*-glycans. The apical high concentration of AGP epitopes in the utricles of *C. fragile* and *C. vermilara* (Estevez et al. 2009 and this study, respectively) suggests a relationship with apical cell expansion in the tip growing cells, as was demonstrated for the moss AGP1 in *Physcomitrella* protonemal growth (Lee et al. 2005). Experiments regarding the biological function of HRGP-like polymers in *Codium* cell walls are in progress to test the effect of the addition of AGP-binding probes on the utricle growth.

Proposed cell-wall model. Based on the preliminary analysis of cell-wall fractions obtained previously from the coenocytic green seaweed *C. vermilara* (Ciancia et al. 2007) together with the carbohydrate analysis of the final residue RW2 (Table S1 and Fig. 5a), it was possible to estimate the total amounts of β-(1 → 4)-D-mannans and SPs (see Materials and Methods for details). In *C. vermilara*, SPs include several polysaccharides with a variety of structures ranging from pyruvylated arabinogalactan sulfates and pyruvylated galactan sulfates to pyranosic arabinan sulfates (Ciancia et al. 2007). Overall, cell walls in *C. vermilara* are composed of ~32% (w/w) of β-(1 → 4)-D-mannans and ~12% (w/w) of sulfated polymers (Table S1 and Fig. 5a). In *C. fragile*, these values were 31% and 9% (w/w), respectively (Estevez et al. 2009), showing similar mannan content and somewhat lower SP content (Table S1 and Fig. 5a). The total estimated amount of cell wall per dry weight is similar in both *C. fragile* (40% w/w) and *C. vermilara* (44% w/w).

Based on the immunolabeling and chemical imaging results (Figs. 2–4), a preliminary model for the utricle cell walls in *C. vermilara* is proposed (Fig. 5b). A sandwich structure with two boundary zones of β-(1 → 4)-D-mannans and HRGP-L epitopes, comprising AGPs and extensins, and a central layer rich in SPs were detected. Based on the results from Estevez et al. (2009), a cell-wall model for *C. fragile* is also included (Figs. 5c and S3, in the supplementary material). The overall cell-wall polymer arrangement of the SPs, HRGP-L epitopes, and β-mannans in *C. vermilara* utricles is different from those present in *C. fragile*, in spite of being phylogenetically very close. In the walls of *C. fragile*, mannans and HRGPs are distributed in a very wide internal layer, and only a narrow external layer was observed, whereas in both seaweeds, SPs form an amorphous middle layer (Fig. 5, b and c).

Until now, there has been no other cell-wall model for any coenocytic algae, and a detailed

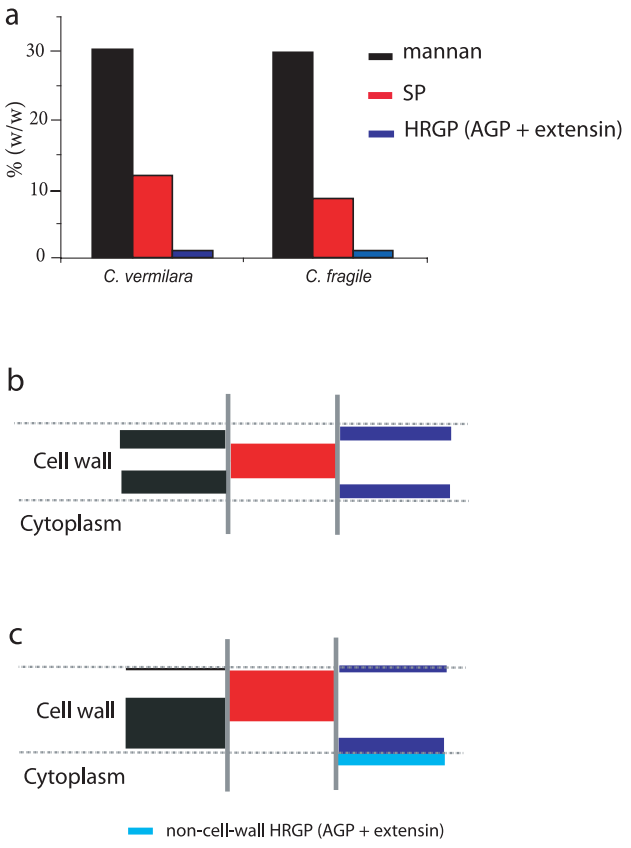

FIG. 5. Cell-wall polymer content and proposed models for *Codium vermilara* and *C. fragile*. (a) Polymer content in both *C. fragile* and *C. vermilara* walls based on chemical analysis made on cell-wall fractions (Table S1, see supplementary material for analysis of *C. vermilara* and Estevez et al. 2009 for analysis of *C. fragile*). (b) Proposed model of the utricle cell wall for *C. vermilara* including the in situ distribution of β-(1 → 4)-D-mannans, SPs, and HRGP-L epitopes. A comparison with *C. fragile* utricle cell wall is included in (c). Mucron cell-wall structure in *C. fragile* is described in Figure S3 (see supplementary material).

picture is available only for the cosmopolitan green macroalga *Ulva* (Bobin-Dubigeon et al. 1997). Even though it is difficult to make a fair comparison between laminar *Ulva* and coenocytic *Codium* thalli structures, certain homologies are shared in their cell-wall polymer properties. Cell-wall polysaccharides in *Ulva* consist of the following: (1) water-soluble xylo-glucurono-rhamnan sulfates (called ulvans) and glucuronan polymers homologous to the negatively charged SPs present in *Codium* walls, and (2) alkali-soluble glucoxylan and amorphous α-cellulose (Lahaye et al. 1994, 1996) that are comparable to β-mannans described previously as both share a β-(1 → 4) backbone with a putative structural role in these cell walls. Ulvans and SPs are both concentrated in the intercellular spaces and middle zone of the cell wall, respectively, whereas neutral β-(1 → 4) polysaccharides are located in the inner part of the cell walls and in the cell surface (Fig. 5, b–c, and Bobin-Dubigeon et al. 1997).

CONCLUSION

Based on this and on previous studies (Bilan et al. 2007, Ciancia et al. 2007, Farias et al. 2008, Estevez et al. 2009), it is evident that *Codium* has developed a unique cell-wall chemistry and architecture when compared with the cellulose-rich cell walls present in land plants and in other green algae (Popper 2008). *Codium* lacks the major polymers typically found in the plant cell walls, such as cellulose, mixed glucans, pectins, xylans, and xyloglucans (Bilan et al. 2007, Ciancia et al. 2007, Farias et al. 2008, Estevez et al. 2009). This green seaweed only shares with some groups of land plants the presence of high quantities of β-mannans (e.g., eusporangiate pteridophytes) and HRGP-L in their cell walls (Ciancia et al. 2007, Popper 2008, Estevez et al. 2009). More seaweed cell-wall models are needed to understand the biological relevance of the polymer chemistry and their arrangements on the cell walls in different thalli types (e.g., uni- or multiseriate filaments, cylindrical, laminar, coenocytic, and massive structures, etc.) in terms of biomechanical properties, fitness and survival, reproduction strategies, and so forth.

The authors gratefully acknowledge C. Somerville for providing most of the antibodies used in this study and also making available to J. M. E. the infrastructure of Carnegie Institution of Washington (Stanford University). Without his support, this work would have not been possible. The authors also thank Paul Dupree for the carbohydrate gel electrophoresis experiment and M. C. Martin for help with the SR–FTIR microspectroscopy analysis (ALS, Berkeley, CA). The Advanced Light Source is supported by the Director, Office of Science, Office of Basic Energy Sciences, of the U.S. Department of Energy under Contract No. DE-AC02-05CH11231. This research was funded by FONCYT (PICT 2006-0983) to J. M. E., and University of Buenos Aires (UBACyT X421 and G048) and National Research Council of Argentina, CONICET (PIP 5699) to M. C.

Ahmed, A. E. R. & Labavitch, J. M. 1977. A simplified method for accurate determination of cell wall uronide content. *J. Food Biochem.* 1:61–365.

Aquino, R. S. & Landeira-Fernandez, A. M. 2005. Occurrence of sulfated galactans in marine angiosperms: evolutionary implications. *Glycobiology* 15:11–20.

Bauer, S., Vasu, P., Persson, S., Mort, A. J. & Somerville, C. R. 2006. Development and application of a suite of polysaccharide-degrading enzymes for analyzing plant cell walls. *Proc. Natl. Acad. Sci. U.S.A.* 103:11417–22.

Bilan, M. I., Vinogradova, E. V., Shashkov, A. S. & Usov, A. I. 2007. Structure of a highly pyruvylated galactan sulfate from the pacific green alga *Codium yezoense* (Bryopsidales, Chlorophyta). *Carbohydr. Res.* 342:586–96.

Bobin-Dubigeon, C., Lahaye, M., Guillon, F., Barry, J. L. & Gallant, D. J. 1997. Factors limiting the biodegradation of *Ulva* sp cell-wall polysaccharides. *J. Sci. Food Agric.* 75:341–51.

Boraso de Zaixso, A. L. 2004. Marine Chlorophyta of Argentina. *Hist. Nat. (Segunda Ser.)* III:95–119.

Chanzy, H. D., Grosrenaud, A., Vuong, R. & Mackie, W. 1984. The crystalline polymorphism of mannan in plant cell walls and after recrystallisation. *Planta* 161:320–9.

Ciancia, M., Quintana, I., Vizcarguenaga, M. I., Kasulin, L., Dios, A., Estevez, J. M. & Cerezo, A. S. 2007. Polysaccharides from the green seaweeds *Codium fragile* and *C. vermilara* with controversial effects on hemostasis. *Int. J. Biol. Macromol.* 41:641–9.

Dhugga, K. S., Barreiro, R., Whitten, B., Stecca, K., Hazebroek, J., Randhawa, G. S., Dolan, M., Kinney, A. J., Tomes, D. & Nichols, S. 2004. Guar seed betamannan synthase is a member of the cellulose synthase super gene family. *Science* 303:363–6.

Domozych, D. S. 2007. Exopolymer production by the green alga *Penium margaritaceum*: implications for biofilm residency. *Int. J. Plant Sci.* 168:763–74.

Domozych, D. S. & Domozych, C. R. 1993. Mucilage processing and secretion in the green alga *Closterium*. II. Ultrastructure and immunochemistry. *J. Phycol.* 29:659–67.

Domozych, D. S., Lambiasse, L., Kiemle, S. N. & Gretz, M. R. 2009. Cell-wall development and bipoalr growth in the desmid *Penium margaritaceum* (Zygnematophyceae, Streptophyta). Asymmetry in a symmetric word. *J. Phycol* 45:879–93.

Eder, M., Tenhaken, R., Driouich, A. & Lütz-Meindl, U. 2008. Occurrence and characterization of arabinogalactan-like proteins and hemicelluloses in *Micrasterias* (Streptophyta). *J. Phycol.* 44:1221–34.

Ender, F., Godl, K., Wenzl, S. & Sumper, M. 2002. Evidence for autocatalytic cross-linking of hydroxyproline-rich glycoproteins during extracellular matrix assembly in *Volvox*. *Plant Cell* 14:1147–60.

Estevez, J. M., Ciancia, M. & Cerezo, A. S. 2004. The system of galactans of the red seaweed, *Kappaphycus alvarezii*, with emphasis on its minor constituents. *Carbohydr. Res.* 339:2575–92.

Estevez, J. M., Fernández, P. V., Kasulin, L., Dupree, P. & Ciancia, M. 2009. Chemical and in situ characterization of macromolecular components of the cell walls from the green seaweed *Codium fragile*. *Glycobiology* 19:212–28.

Estevez, J. M., Kiesliszewski, M. J., Khitrov, N. & Somerville, C. 2006. Characterization of synthetic hydroxyproline-rich proteoglycans with AGP- and extensin-motifs in *Arabidopsis*. *Plant Physiol.* 142:458–70.

Estevez, J. M., Leonardi, P. & Alberghina, J. 2008. Cell wall carbohydrate-epitopes in the green algae *Oedogonium bharuchae* f. *minor* (Oedogoniales, Chlorophyta). *J. Phycol.* 44:1257–68.

Farias, E. H. C., Pomin, V. H., Valente, A. P., Nader, H. B., Rocha, H. A. O. & Mourao, P. A. S. 2008. A preponderantly 4-sulfated, 3-linked galactan from the green alga *Codium isthmocladum*. *Glycobiology* 18:250–9.

Fukushi, Y., Otsuru, O. & Maeda, M. 1988. The chemical structure of the D-xylan from the main cell wall constituents of *Bryopsis maxima*. *Carbohydr. Res.* 182:313–20.

Guiry, M. D. & Guiry, G. M. 2009. *AlgaeBase*. Worldwide electronic publication, National University of Ireland, Galway. Available at: http://www.algaebase.org.

Hallmann, A. 2006. The pherophorins: common, versatile building blocks in the evolution of extracellular matrix architecture in Volvocales. *Plant J.* 45:292–307.

Hames, B. D. & Rickwood, D. [Eds.] 1990. *Gel Electrophoresis of Proteins, A Practical Approach*, 2nd ed. Oxford University Press, New York, 404 pp.

Handford, M. G., Baldwin, T. C., Goubet, F., Prime, T. A., Miles, J., Yu, X. & Dupree, P. 2003. Localization and characterization of cell wall mannan polysaccharides in *Arabidopsis thaliana*. *Planta* 218:27–36.

Hay, M. 1997. Synchronous mass spawning: when timing is everything. *Science* 275:1080–1.

Hicks, G. R., Hironaka, C. M., Dauvillee, D., Funke, R. P., D'Hulst, C., Waffenschmidt, S. & Ball, S. G. 2001. When simpler is better. Unicellular green algae for discovering new genes and functions in carbohydrate metabolism. *Plant Physiol.* 127:1334–8.

Huizing, H. J., Rietema, H. & Sietsma, J. H. 1979. Cell wall constituents of several siphonaceous green algae in relation to morphology and taxonomy. *Br. Phycol.* 14:25–32.

Kloareg, B. & Quatrano, R. S. 1988. Structure of the cell wall of marine algae and ecophysiological functions of the matrix polysaccharides. *Oceanogr. Mar. Biol. Annu. Rev.* 26:259–315.

Knox, J. P., Linstead, P. J., Peart, J., Cooper, C. & Roberts, K. 1991. Developmentally-regulated epitopes of cell surface arabinogalactan-proteins and their relation to root tissue pattern formation. *Plant J.* 1:317–26.

Koepsell, H. J. & Sharpe, E. S. 1952. Microdetermination of pyruvic and α-ketoglutaric acids. *Arch. Biochem. Biophys.* 38:443–9.

Krishnamurthy, K. V. 1999. Transmission electron microscopic cytochemistry. *In* Krishnamurthy, K. V. [Ed.] *Methods in Cell Wall Cytochemistry*. CRC Press, Tiruchirappalli, India, pp. 177–226.

Lahaye, M., Jegou, D. & Buleon, A. 1994. Chemical characteristics of insoluble glucans from the cell wall of the marine green algae *Ulva lactuca* (L.) Thuret. *Carbohydr. Res.* 262:115–25.

Lahaye, M., Ray, B., Baumberger, S., Quemener, B. & Axelos, M. A. V. 1996. Chemical characterisation and gelling properties of cell-wall polysaccharides from species of *Ulva* (Ulvales, Chlorophyta). *Hydrobiologia* 326/327:473–80.

Lee, K. J. D., Sakata, Y., Mau, S. L., Pettolino, F., Bacic, A., Quatrano, R. S., Knight, C. D. & Knox, P. 2005. Arabinogalactan proteins are required for apical cell extension in the moss *Physcomitrella patens*. *Plant Cell* 17:3051–65.

Les, D. H., Cleland, M. A. & Waycott, M. 1997. Phylogenetic studies in alismatidae II: evolution of marine angiosperms (seagrasses) and hydrophily. *Syst. Bot.* 22:443–63.

Liepman, A. H., Nairn, C. J., Willats, W. G. T., Sørensen, I., Roberts, A. W. & Keegstra, K. 2007. Functional genomic analysis supports conservation of function among cellulose synthase-like a gene family members and suggests diverse roles of mannans in plants. *Plant Physiol.* 143:1881–93.

Liepman, A. H., Wilkerson, C. G. & Keegstra, K. 2005. Expression of cellulose synthase-like (Csl) genes in insect cells reveals that CslA family members encode mannan synthases. *Proc. Natl. Acad. Sci. U.S.A.* 102:2221–6.

Lutz-Meindl, U. & Brosch-Salomon, S. 2000. Cell wall secretion in the green alga *Micrasterias*. *J. Microsc.* 198:208–17.

Morrison, I. M. 1988. Hydrolysis of plant cell walls with trifluoroacetic acid. *Phytochemistry* 27:1097–101.

Ponce, N. M., Pujol, C. A., Damonte, E. B., Flores, M. L. & Stortz, C. A. 2003. Fucoidans from the brown seaweed *Adenocystis utricularis*: extraction methods, antiviral activity and structural studies. *Carbohydr. Res.* 338:153–65.

Popper, A. Z. 2008. Evolution and diversity of green plant cell walls. *Curr. Opin. Plant Biol.* 11:286–92.

Popper, Z. A. & Fry, S. C. 2003. Primary cell wall composition of bryophytes and charophytes. *Ann. Bot.* 91:1–12.

Prado Fernández, J., Rodríguez-Vazquez, J. A., Tojo, E. & Andrade, J. M. 2003. Quantitation of κ-, ι-, and λ-carrageenans by mid-infrared spectroscopy and PLS regression. *Anal. Chim. Acta* 480:23–37.

Ram, M. & Babbar, S. B. 2002. Transient existence of life without a cell membrane: a novel strategy of siphonous seaweed for survival and propagation. *Bioessays* 24:588–90.

Santos, J. A., Mulloy, B. & Mourao, P. A. S. 1992. Structural diversity among sulfated L-galactans from Ascidians (tunicates): studies on the species *Ciona intestinalis* and *Herdmania monus*. *Eur. J. Biochem.* 204:669–77.

Smallwood, M., Beven, A., Donovan, N., Neill, S. J., Peart, J., Roberts, K. & Knox, J. P. 1994. Localization of cell wall proteins in relation to the developmental anatomy of the carrot root apex. *Plant J.* 5:237–46.

Spurr, A. R. 1969. A low-viscosity epoxy embedding medium for electron microscopy. *J. Ultrastruct. Res.* 26:31–43.

Stortz, C. A. & Cerezo, A. S. 2000. Novel findings in carrageenans, agaroids and ''hybrids'' red seaweed galactans. *Curr. Top. Phytochem.* 4:121–34.

Verbruggen, H., Leliaert, F., Maggs, C. A., Shimada, S., Schils, T., Provan, J., Booth, D., et al. 2007. Species boundaries and phylogenetic relationship within the green algal genus *Codium* (Bryopsidales) based on plastid DNA sequences. *Mol. Phylogenet. Evol.* 44:240–54.

Vilela-Silva, A. C. E. S., Castro, M. O., Valente, A. P., Biermann, C. H. & Mourao, P. A. S. 2002. Sulfated fucans from the egg jellies of the closely related sea urchins *Strongylocentrotus droebachiensis* and *Strongylocentrotus pallidus* ensure species-specific fertilization. *J. Biol. Chem.* 277:379–87.

Yamagishi, T., Hishinuma, T. & Kataoka, H. 2004. Novel sporophyte-like plants are regenerated from protoplasts fused between sporophytic and gametophytic protoplasts of *Bryopsis plumosa*. *Planta* 219:253–60.

Yariv, J., Rapport, M. M. & Graf, L. 1962. The interaction of glycosides and saccharides with antibody to the corresponding phenylazo glycoside. *Biochem. J.* 85:383–8.

Yates, E. A., Valdor, J. F., Haslam, S. M., Morris, H. R., Dell, A., Mackie, W. & Knox, J. P. 1996. Characterization of carbohydrate structural features recognized by anti-arabinogalactan-protein monoclonal antibodies. *Glycobiology* 6:131–9.

Supplementary Material

The following supplementary material is available for this article:

Figure S1. FTIR spectra of the highly sulfated extract V1. Comparison with the nonsulfated mannan-rich RW2 residue is included to identify diagnostic absorbance bands exclusive for sulfate groups. FTIR, Fourier transform infrared; RW2, residue obtained after hot-water extractions.

Figure S2. Immunodot-blot screening of HRGP-L epitopes (AGPs and extensins) on cell-wall fractions V1 and V2 isolated from *Codium vermilara* (see also Table S1 in the supplementary material). Only positive labeling of antibodies against HRGP-L epitopes present in V1-V2 were included in the figure. AGPs, arabinogalactan proteins; HRGP-L, hydroxyproline-rich glycoprotein-like.

Figure S3. Proposed cell-wall model at the utricle tip (named as mucron) for *Codium fragile*.

Table S1. Mannan and sulfated polymer contents in the cell walls of *Codium vermilara*.

This material is available as part of the online article.

Please note: Wiley-Blackwell are not responsible for the content or functionality of any supplementary materials supplied by the authors. Any queries (other than missing material) should be directed to the corresponding author for the article.